ABSOLUTE FERROUS ABSORPTION BAND STRENGTH IN THE LUNAR FELDSPATHIC HIGHLANDS TERRANE FROM THE MOON MINERALOGY MAPPER. Peter J. Isaacson[1], Noah E. Petro[2], Carlé M. Pieters[3], Sebastien Besse[4], Joseph W. Boardman[5], Roger N. Clark[6], Robert O. Green[7], Sarah Lundeen[7], Erick Malaret[8], Stephanie McLaughlin[4], Jessica M. Sunshine[4], Lawrence A. Taylor[9], and the M^3 Team, [1]Hawaii Institute of Geophysics and Planetology, University of Hawaii, Manoa, Honolulu, HI, 96822, [2]NASA GSFC, [3]Brown University, [4]Univ. of MD, [5]AIG, [6]USGS Denver, [7]JPL, [8]ACT, [9]Univ. of Tenn., [isaacson@higp.hawaii.edu].

Introduction: The feldspathic highlands terrane (FHT) is one of three major lunar crustal terranes defined by Jolliff et al. [1] based primarily on orbital estimates of surface bulk chemistry [2, 3]. The FHT is characterized by low FeO and Th abundance. Orbital chemical assessments and subsequent mineralogical analyses of central peaks within the FHT [4, 5] indicate that the region is anorthositic to substantial depth.

Significance of ferrous absorption features. Visible to near-infrared (VNIR) reflectance spectra of common lunar minerals exhibit absorption features near 1 μm caused by Fe^{2+} ions in mineral structural sites [e.g., 6]. The strength and position of this feature is controlled by a variety of factors, including mineralogy, mineral composition, grain size, degree of space weathering, etc.. This feature is one of the primary means for evaluating lunar mineralogy with VNIR observations, and its strength has direct implications for assessments of mineralogy and chemistry. The anorthositic nature of the FHT is expected to produce relatively weak 1 μm absorption features, as anorthositic materials contain low abundances of minerals with strong 1 μm absorption features (e.g. pyroxene, olivine). Analysis of the weak absorption features in the FHT offer the opportunity to "benchmark" the 1 μm absorption features detected by the Moon Mineralogy Mapper (M^3) and enable more accurate characterizations of mineralogy and composition on a global scale with the M^3 dataset.

M^3 Operational Periods and Ground Truth Correction. Over the course of the Chandrayaan-1 mission, numerous operational challenges were encountered that led to M^3 being operated well outside its intended range of temperature and surface illumination conditions, which had direct implications for the character of the acquired data. In this work, we will refer to two periods: OP1B and OP2C1. OP1B was marked by relatively low sun angles and detector temperatures, and by low signal but correspondingly low noise levels. OP2C1 was marked by high sun angles and detector temperatures, and data with high signal levels but also elevated noise levels. These operational periods are discussed in far greater detail by [7]. The M^3 team also developed a ground truth correction based on known properties of lunar soils from laboratory analyses. The ground truth correction is described in the M^3 data product SIS document provided with the M^3 PDS archive [8] and in the M^3 data user's tutorial available at http://m3.jpl.nasa.gov/m3data.html.

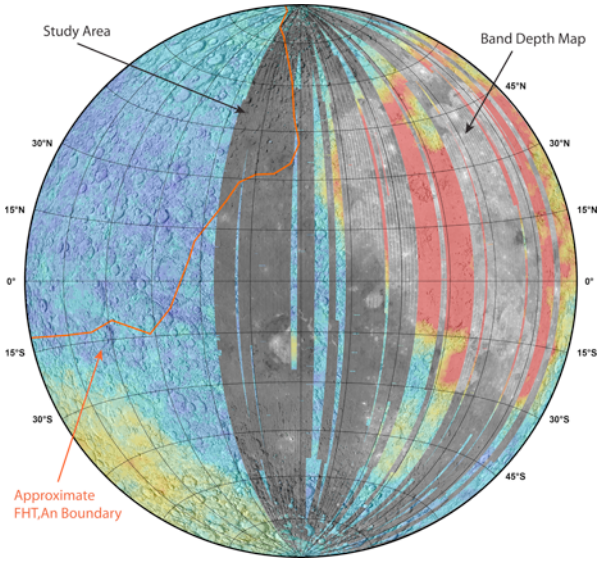

Fig. 1: Illustration of study region and example results. Basemap is Lunar Prospector 0.5° derived Fe abundance [9] over the USGS shaded relief map. The greyscale overlay is the integrated band depth map for OP1B (see Methods), demonstrating the weak absorption features detected in the region. The approximate boundaries of the most feldspathic portion of the FHT (FHT,An) are illustrated. The study region is where the FHT,An and band depth map intersect. Lambert Azimuthal Equal Area projection centered on 90°W.

Study Region and Methods: In order to assess the observed band strength over the range of conditions experienced by M^3, we restricted our analyses to regions in which data were acquired during both OP1B and OP2C1. This produced a study area located on the western limb and eastern farside of the Moon. To quantify the band strength, we developed two spectral parameters. One parameter is an integrated band depth that summed the absorption strength between 770 nm and 1100 nm. Such integrated band depths are not necessarily direct proxies for maximum absorption strength, so we also used a single channel band depth at 970 nm. The study region is illustrated in Fig. 1. Both band depth parameters were calculated relative to a linear continuum slope over the 1 μm region. We

mapped these parameters across the study region for OP1B and OP2C1 data, both with and without the ground truth correction applied, for a total of four possible "scenarios". Mean values for each scenario were calculated. As regions at high latitude often exhibit artifacts due to low signal levels and extreme illumination conditions, we calculated mean values for the study area for a series of maximum latitude cutoffs (full region, max. of 70°N, max 65°N, and max. 60°N).

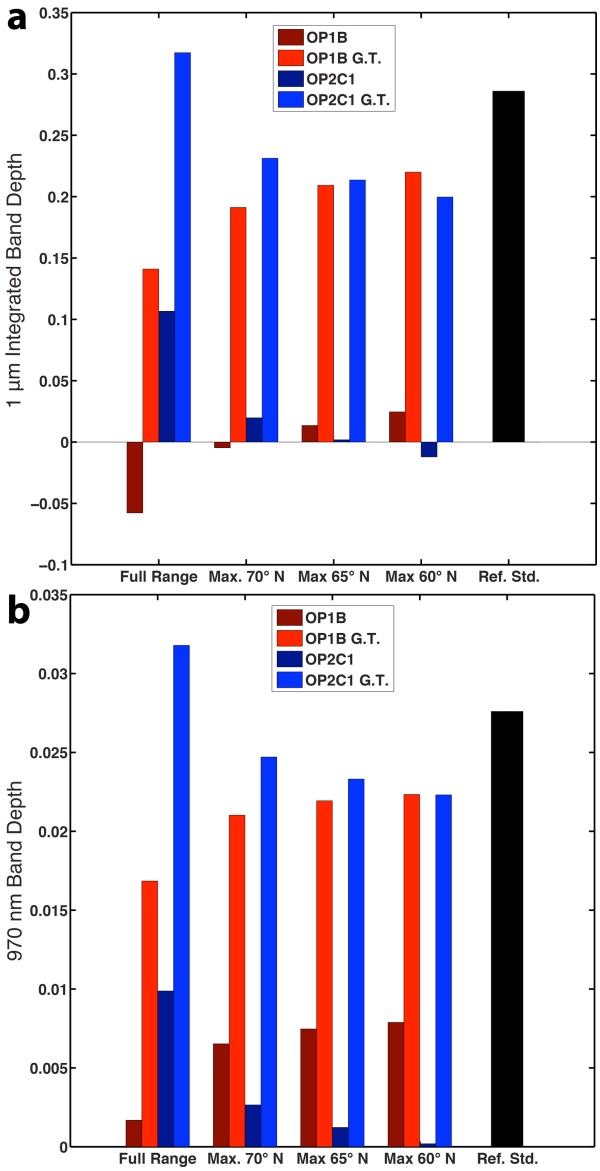

Fig. 2: Comparison of mean band strengths (a, integrated, b, single channel) from the study area and the reference standard (Apollo 16 soil) spectrum. Results are presented for a series of maximum latitude cutoffs and both with ("G.T.") and without the ground truth correction, as discussed in the text. Note the similarity between OP1B G.T., OP2C1 G.T., and the Ref. Std., particularly for lower latitude cutoffs.

Results: The mean band strengths (using both parameters) measured for the study region for the four scenarios and various latitude cutoffs are illustrated in Fig. 2. The band strengths are also compared to the parameter value of the laboratory reference standard (62231 soil [10]) used in the ground truth correction.

Discussion and Implications: The integrated and single-channel parameters produce overall consistent trends. The FHT region studied exhibits weak absorption features, consistent with a highly feldspathic composition. Clear differences in band strength are observed between OP1B and OP2C1, especially without the ground truth correction. As these analyses cover identical terrain, the differences result from different properties of the M^3 dataset under variable operational conditions. Considering the lower latitude cutoffs (removing artifacts primarily associated with extreme latitudes), it is clear that the ground truth correction brings the observed band strengths into closer agreement between the two periods, as well as with the reference standard. The difference between the M^3 observations and the reference standard is not unexpected, as the reference standard comes from the Apollo 16 site whereas the M^3 measurements come from the western limb and farside. While both are highly feldspathic, they are not necessarily compositionally identical [e.g., 11, 12]. The ground truth correction clearly makes the observed band strengths more consistent between OP1B and OP2C1. However, the ground truth correction derived for the M^3 dataset only addresses wavelengths below 1500 nm. The variable band strengths observed in M^3 data and the need for any ground truth corrections must be carefully weighed by any researchers conducting regional or global analyses with the M^3 dataset, particularly those in which mature lunar soils with weak absorption features dominate. These issues are discussed further by [13].

Acknowledgments: M^3 science validation is supported by NASA contract #NNM05AB26C. M^3 is supported as a NASA Discovery Program mission of opportunity. The M^3 team is grateful to ISRO for the opportunity to be a guest instrument on Chandrayaan-1.

References: [1] Jolliff, B.L. et al. (2000) *JGR*, **105**, 4197-4216, 10.1029/1999JE001103. [2] Lucey, P.G. et al. (1998) *JGR*, **103**, 3679–3699, 10.1029/97JE03019. [3] Lawrence, D.J. et al. (1998) *Science*, **281**, 1484, 10.1126/science.281.5382.148. [4] Tompkins, S. and Pieters, C.M. (1999) *MAPS*, **34**, 25-41, 10.1111/j.1945-5100.1999.tb01729.x. [5] Cahill, J.T.S. et al. (2009) *JGR*, **114**, 10.1029/2008je003282. [6] Burns, R.G. (1993) *Mineralogical applications of crystal field theory*. [7] Boardman, J.W. et al. (2011) *JGR*, **116**, 10.1029/2010JE003730. [8] Lundeen, S. et al., Moon Mineralogy Mapper Data Product Software Interface Specification. 2011, NASA Planetary Data System. [9] Lawrence, D.J. et al. (2002) *JGR*, **107**, 5130, 10.1029/2001je001530. [10] Pieters, C.M. (1999) *Workshop on New Views of the Moon II*, 8025. [11] Warren, P.H. (2005) *MAPS*, **40**, 477, 10.1111/j.1945-5100.2005.tb00395.x. [12] Korotev, R.L. et al. (2003) *GCA*, **67**, 4895-4923, 10.1016/j.gca.2003.08.001. [13] Isaacson, P.J. et al. (Submitted) *JGR*.